ORIGINAL PAPER

A software approach for identifying the effect of dental caries on dentin–enamel junction

BOGDAN MIHAI GĂLBINAŞU[1], HORIA OCTAVIAN MANOLEA[2], IOANA MATEI[3], MIHAI ANDREI[4], MIHNEA IOAN NICOLESCU[5,6]

[1]Discipline of Dental Prosthesis Technology and Dental Materials, Faculty of Dental Medicine, Carol Davila University of Medicine and Pharmacy, Bucharest, Romania

[2]Department of Dental Materials, Faculty of Dentistry, University of Medicine and Pharmacy of Craiova, Romania

[3]Endodontics Resident, Titu Maiorescu University, Bucharest, Romania

[4]Discipline of Embryology, Faculty of Dental Medicine, Carol Davila University of Medicine and Pharmacy, Bucharest, Romania

[5]Discipline of Histology and Regenerative Dentistry, Faculty of Dental Medicine, Carol Davila University of Medicine and Pharmacy, Bucharest, Romania

[6]Laboratory of Radiobiology, Victor Babeş National Institute of Pathology, Bucharest, Romania

Abstract

Dental decay is the most prevalent oral disease worldwide since more than 2.4 billion people suffer from caries of permanent teeth. Therefore, any details about its progression into the hard-dental tissues could contribute to unravelling the mechanisms underlying this process. We have analyzed dental tissue sections with and without caries in order to detect structure differences corelating them with clinical aspects observable from the tooth surface. Our working hypothesis was based on finding a link between the process of tertiary dentin laying (as a response to coronal caries) and the subsequent obliteration of dentin tubules. We have selected *N*=10 extracted teeth with/without coronal caries, resin-embedded and sectioned them. A specific software was used to digitally quantify the density of unobliterated dentin tubules reaching the dentin–enamel junction (DEJ), considering as positive threshold criteria the presence of the odontoblast process inside the analyzed tubule. This study showed the differences between the healthy and carious-affected hard-dental coronal tissues. More odontoblast processes reached the DEJ in unaffected teeth. Using specific software, we have quantified their density decrease near a lesion. We have studied the dynamics of the carious study and measured the consequent structural modifications of the dentin. In conclusion, there is a significant difference between the number of dentin tubules containing odontoblast processes that reach the DEJ in healthy/altered tissues. The tooth reacts not only by production of tertiary dentin to protect the pulp chamber, but also by obliteration of dentin tubules, thus reducing the number of odontoblast processes reaching the DEJ. This pilot study could serve as the starting point in developing a dedicated software that could deliver a personalized pattern for decay progression by analyzing one single tooth and extrapolate the result to all the patient's remaining ones.

Keywords: dental caries, dentin–enamel junction, dental research, software, odontoblasts.

Introduction

The main element of protection against dental caries is the enamel. This is designed to withstand various physical and chemical challenges. However, there are certain instances in which this resistance can be overcome. The enamel may have a lower resistance to begin with, in which case there is a structure deficit. However, enamel can resist cavity attack if its chemical structure is stable and intact. Numerous histological studies were at the basis of the idea that a caries process is not simply a progressive demineralization, but an alternant process of destruction and repair. The first modification that we may observe at the beginning of a dental caries is the optical properties alteration. The enamel, which is usually translucent, is starting to show small, chalk white spots at the surface. These constitute the first clinical sign of demineralization, and it can easily be overlooked if the objective examination is superficial [1].

During this stage, we may observe an enlargement of interprismatic spaces, modifications of the crystal orientation and appearance of atypical shapes and alteration of the organic matrix leading to increased tissue permeability [2].

The penetration of saliva components into enamel is possible after demineralization and dissolution of certain mineral elements in the dental structure. Fejerskov & Kidd [3] appreciate there is a delimitation between stopping the acid attack and remineralization. They claim that stopping the acid attack does not necessarily imply tissue remineralization and the so-called remineralization aspect comes from covering the structure defect with a film of saliva.

In the first moment of the acid attack, the modifications are produced in the nucleus of the prism and only afterwards on its walls. This phenomenon appears due to the difference between the walls' richer mineralization and the reduced one of the nucleus [3]. Finally, the acid attack enters the enamel sheath which leads to the appearance of spaces

without crystals and later without prisms. These spaces confluence and determine the collapse of surface enamel forming a pit or a cavity. Several histological areas of caries in the enamel have also been described, starting from the vicinity of healthy enamel: translucent area, dark area, the body of the lesion and surface area. Moreover, the surface area arose numerous controversies, being almost entirely unaffected, thus consisting entirely of enamel. An explanation for the existence of this layer was attributed [4] to the presence of bacterial plaque over the lesion which performs the role of a barrier. This barrier retains calcium, phosphate and fluorine ions released by enamel demineralization or from the saturated solution from the plaque.

Incipient caries lesions usually evolve after the pattern of the four characteristic areas described above. In their evolution, incipient caries lesions also demineralize the surface area from the outside inwards and begin to advance rapidly towards the dentin and dental pulp. From a histological point of view, they first appear to penetrate the enamel through Retzius lines, then along the interprismatic substance and finally inside enamel prisms.

Aim

We aimed to assess whether the carious process cause changes at the level of odontoblast processes reaching the dentin–enamel junction (DEJ).

⊡ Materials and Methods

We selected *N*=10 human cusp teeth (premolars and molars) extracted from both maxilla and mandible, teeth that we labeled D1 to D10, with the following correspondence in *World Dental Federation* system: D1 (2.8.), D2 (3.4.), D3 (2.4.), D4 (2.8.), D5 (1.8.), D6 (2.8.), D7 (3.8.), D9 (1.8.), and D10 (4.8.).

All the biological samples have been obtained in an authorized dental office, following the extractions needed by previously established treatment plans, with the informed consent of all patients. The teeth were then processed in the preclinical research facilities of Faculty of Dental Medicine, Carol Davila University of Medicine and Pharmacy, Bucharest, Romania.

Firstly, we have photographically documented them using a Nikon D7200 professional camera (with APS-C sensor, 1.5 crop factor, Nikon, Tokyo, Japan), with a macro lens from Sigma Corporation (Kawasaki, Japan) and a MF18 ring flash (Nissin Digital, Japan) as external light.

After carefully analyzing the quality and the accuracy of the photos, we embedded the teeth in an epoxy resin (EpoFix, Struers GmbH, Germany) (Figure 1). This specific resin was chosen due to its transparency (with a refractive index close to that of the glass – approximately 1.51) and lower setting time (earning a suitable hardness for sectioning with the circular diamond blade, without altering the interplanar parallelism of the dental structures). The resin-embedding process followed the protocol indicated by the manufacturer (a 15:2 volumetric ratio resin/hardener). We stirred vigorously and prepared a mixture of 75 mL resin and 10 mL hardener, which we used for mounting all of our specimens. We have inserted a compatible metal holder in each resin block, to serve as a support for the sectioning step, to be easily positioned and perfectly cut

by the rotating blade. The metal holder alloy was compatible with the two components of the resin and was also inert to the polymerization. After 12 hours, the specimens were embedded correctly in the resin blocks. All teeth were embedded in a position that would allow buccal–oral sectioning.
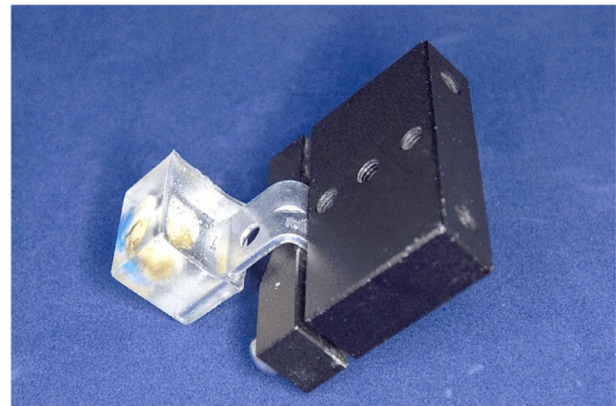

Figure 1 – *Tooth embedded in a transparent epoxy resin, with metal holder.*

We sectioned the samples using the Smart Cut 6010 (UKAM Industrial Superhard Tools, Valencia, CA, USA). The sectioning machine operates with a passive cooling system, which is executed by passing the disc through a tank in which the cooling liquid is found. In cutting process for our samples, we used the cooling and lubricating fluid recommended by the manufacturer. Sectioning of the resin blocks was performed with a controlled weight applied on a rod system, mounted parallel to the arm on which the grip was mounted together with the block that underwent the cutting. The weight that we applied was between 400–500 g. The cutting speed was set to 1000–1200 rpm.

We used a diamond disc (Ukam, # 4BC1) and a steel one with a diamond outer edge (Ukam, Series 15 LCU) to obtain the desired sections. The resulted slices of dental tissue embedded in resin had a thickness of about 100 μm. The sections did not require demineralization and could be used as such in the study (Figure 2).
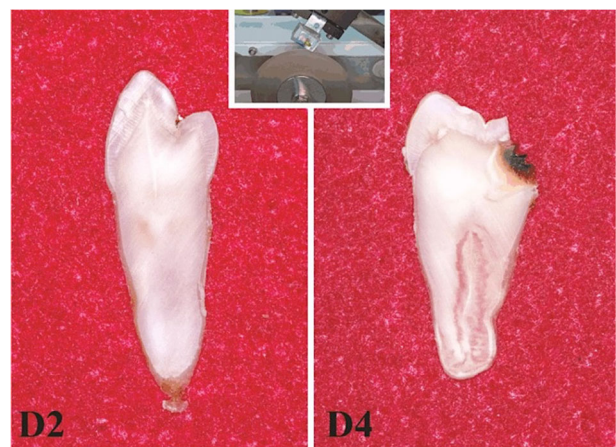

Figure 2 – *Sections of teeth from resin blocks. Note the resin surrounding dental tissue. Left: D2 (healthy tooth); Right: D4 (decayed tooth); Inset: Resin block with tooth during sectioning.*

We examined the sections under a Zeiss Axiostar Plus light microscope (Carl Zeiss, Germany), to which we attached, with the help of an extension tube adapter, the

professional camera described previously. The images were then acquired, processed, and analyzed using specialized software, described below. For image calibration, we used I-SEEING™ (Shanghai Qing Ying E&T LLC, Shanghai, People Republic of China) calibration scales type 2016-48-03, dimensions 60×40×0.2 mm. The pattern that we used was the 5 mm grid type with a 0.2 mm distribution (tolerance ±0.005 mm). Images were captured using magnification of 5×, 10× and 20×, then after analyzing the images with the specimens we decided to use measurements only for images captured with a magnifying power of 10× lens for $n=9$ sections, respectively 5× for $n=1$ of the sections. We calibrated the dimension of all the images we obtained, correlating the number of pixels with their correspondent in millimeters, respectively microns. We have chosen to use a scaling bar of 500 µm, further used for measuring the density of the identified odontoblastic processes inside the dentin tubules.

In order to ease the bioinformatic analysis, it was necessary to increase the differential contrast on the images we have studied. So, they were processed by using the high pass filter combined with the hard-light filter in Adobe Photoshop software version CC 2019 (20.0.0). For our bioinformatic analysis of the images, we used the open-source software Image J, version 1.52.

We have selected a section of 0.2/0.2 mm for all the images. On the 500-µm scale bar, we applied a plot algorithm that generated a graph based on the arithmetic mean of each vertical line of pixels. To align the analyzed section with the orientation of the odontoblast extensions, we used an image rotation script based on two xOy coordinate points. After obtaining the plot graph, we used an algorithm to analyze the maximum points of each graph, to determine the approximate number of extensions on the analyzed section.

Results

In the Figures 3 and 4, we may see the initial photographic documentation of the samples ($N=10$). We may observe on the photographed teeth the absence (Figure 3) or the presence (Figure 4) of the carious lesions, as well as the integrity of the tooth before embedding and sectioning. For each examined tooth, we can observe the morphology of the occlusal surface, a proximal surface and finally the buccal or the oral surface, depending on the particular morphopathological aspects of each of the studied teeth.

After processing the acquired images of the sections, we analyzed them using specialized software and made measurements regarding the number of extensions of the odontoblasts that reached the level of the DEJ in healthy tissue, as well as in carious dentin. The measurements and calibration were performed as described in the methodology section above.

The enhanced light microscopy morphological aspect of the healthy samples that we analyzed (D1, D2, D3, D5, and D9 – Figure 5) may be seen in the left part of the Figure 5. The microscopy images show the morphological aspect of the DEJ, which represents the place where two morphologically and physiologically complementary but structurally different tissues meet. The histological aspect of a normal DEJ is a scalloped line, where tubules parallel to enamel can be observed on the internal side, while the outer enamel–facing counterpart may exhibit small defects like tufts or spindles, or even larger ones – lamellae.

The graphical results offered by the software after the measurements of tubules containing odontoblast processes reaching DEJ on a length of 500 µm may be seen in the right part of the Figure 5 for each of the five teeth examined. All the samples presented a large number of measured odontoblast processes, respectively D1=35, D2=34, D3=37, D5=30, and D9=27.

The enhanced light microscopy morphological aspect of the samples with caries lesions that we analyzed (D4, D6, D7, D8, and D10 – Figure 6) may be seen in the left part of the Figure 6. The microscopy images show that the morphology of these areas is in a permanent evolution in terms of caries attack and consequently different types of dentin can be highlighted. We have chosen teeth with caries distant from the analyzed DEJ, to be able to assess its distant modification. Thus, we noticed an increased obliteration of dentin tubules in their distal part, towards DEJ (as opposed to a putative dentin demineralization in the vicinity of DEJ caries). The graphical results offered by the software after the measurements of tubules containing odontoblast processes reaching DEJ on a length of 500 µm may be seen in the right part of the Figure 6 for each of the five teeth examined. The specimens with caries lesions (D4, D6, D7, D8, and D10 – Figure 6) had fewer odontoblastic processes, respectively D4=15, D6=22, D7=22, D8=18, and D10=20.

In order to help the reader, we made a graphic showing the number of identified odontoblast processes reaching DEJ on a length of 500 µm, where we have chosen to assign green color for healthy teeth and red color for teeth with caries (Figure 7). The average obtained values were 32.6±1.81 extensions/500 µm for teeth decay-free and 19.4±1.33 extensions/500 µm respectively for those with caries (Table 1).

Statistical analysis t-test is a way of identifying significant differences between two populations or arrays; in our case, the differences between the odontoblast processes existing in the healthy tissue and those in carious lesions. t-test is a hypothesis test, to which we set an error of 0.05. Our hypothesis is that healthy teeth have an average of 10 more processes compared to those affected by caries and if the p value is higher than the error, the hypothesis is invalidated. In case the p value is lower, we can further explore our assumption. For the hypothesis to be valid, the equations $t_{Stat} > -t_{Critical\ two\ tail}$ and $t_{Stat} < t_{Critical\ two\ tail}$ must be true. Calculating the values mentioned above, we obtained $t_{Stat}=5.89$ and $t_{Critical\ two\ tail}=2.30$, values that are true for the second equation and also $t_{Stat} > t_{Critical\ two\ tail}$ (1.42<2.30). From those, the t-test analysis confirmed that the number of odontoblastic extensions is greater in the healthy tissue in comparison to those with cavities. In other words, teeth with caries have a larger number of obliterated dentinal tubules, confirming our initial hypothesis, this process being the tooth's response to pathogenic agents. This response is materialized by the formation of tertiary dentin and the subsequent obliteration of the dentinal tubules. For a better understanding of the gathered results, we generated a type t distribution using points from the interval [-4, 4] with a 0.2 distance between them. We labeled the set of identified points as $A=\{-4.0, -3.8, …, 3.8, 4.0\}$. For each of the point in the set, we generated it corresponds a value in the t distribution, based on the same eight freedom degrees previously used in calculating the t-test. The calculation resulted in a B set of points, having the same cardinal as in the A set, representing the points of t distribution.

Using the data from the *B* set of points we generated the graph in Figure 8 to which we added the *t* value obtained after the *t*-test. As it can easily be observed in the graph, the extremities are marked in red, representing the values for which the hypothesis is invalid. Since the *t* value we determined is in-between the acceptable limits of the *t* distribution, we can conclude that our initial hypothesis is validated by the results of the *t*-test.

D1 (2.8) – Occlusal, proximal, oral

D2 (3.4) – Occlusal, buccal, proximal

D3 (2.4) – Occlusal, proximal, oral

D5 (1.8) – Occlusal, buccal, proximal

D9 (1.8) – Occlusal, buccal, proximal

Figure 3 – *Initial photographic documentation of teeth without decays (D1, D2, D3, D5, and D9). Occlusal, proximal, buccal/oral views.*

D4 (2.8) – Occlusal, buccal, proximal

D6 (2.8) – Occlusal, buccal, proximal

D7 (3.8) – Occlusal, buccal, proximal

D8 (1.8) – Occlusal, oral, proximal

D10 (4.8.) – Occlusal, oral, proximal

Figure 4 – *Initial photographic documentation of teeth with decays (D4, D6, D7, D8, and D10). Occlusal, proximal, buccal/oral views.*
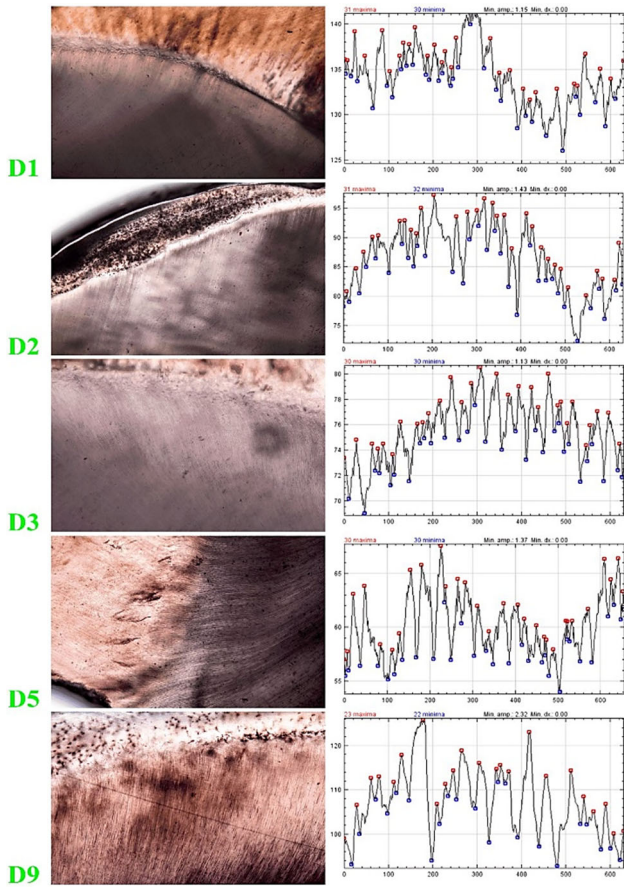
Figure 5 – *Samples of teeth without decays (D1, D2, D3, D5, and D9). Left panels: Enhanced light microscopy; Right panels: Software measurements of tubules containing odontoblast processes reaching dentin–enamel junction on a length of 500 μm.*
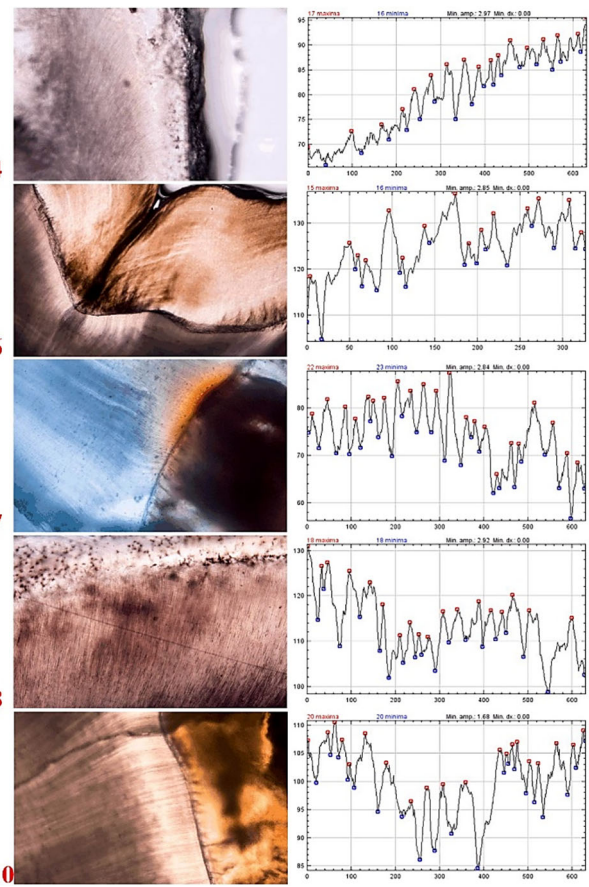

Figure 6 – *Samples of teeth with decays (D4, D6, D7, D8, and D10). Left panels: Enhanced light microscopy; Right panels: Software measurements of tubules containing odontoblast processes reaching dentin–enamel junction on a length of 500 μm. Note: Sections are unstained. The blue color visible at D7 is just an optical effect.*
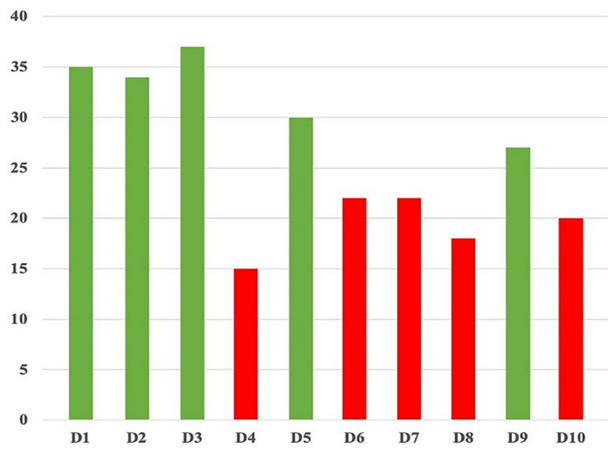

Figure 7 – *Number of identified odontoblast processes reaching dentin–enamel junction on a length of 500 μm. In green – healthy tooth samples, in red – decayed tooth samples.*

Figure 8 – *t-test distribution of samples.*

Table 1 – *Average number of identified odontoblast processes reaching dentin–enamel junction (measured per 500 μm)*

	Healthy teeth	Carious teeth
Average	32.60	19.40
Standard error	1.81	1.33
Median	34.00	20.00
Standard deviation	4.04	2.97

Discussions

After analyzing the results, we confirmed that the number of dental extensions that reach the DEJ in healthy teeth is higher than in the decayed ones.

Our measurements yielded an average density of approximately 32 processes/500 μm in teeth without caries and 19 processes/500 μm near the caries. In a similar study, Maniatopoulos & Smith studied the processes of

odontoblasts using three methods of sample preparation [5]. Even if the difference between our research and the above-mentioned study lies in the number of preparation methods, they identified the extensions from the external third using the first method for all the examined specimens, for a single specimen using the second and with the third method odontoblast processes were not found, but only the fibers that surrounded them.

Another similar study is that of Brännström & Garberoglio [6], who studied the arrangement of the processes and their expansion in dentin, the difference between the two studies being the analysis of the odontoblastic process in terms of their diameter on different areas of dentin. At the same time, they investigated the intra- and extra-canalicular morphology, giving a precise description of all the encountered structures. Both above-mentioned studies have a resolution advantage represented using the electron microscope.

The study of odontoblasts following dental injury carried out by Murray *et al.* is similar by histomorphometry counting [7]. The odontoblasts were counted for each section on a surface of 2112 μm^2 of pulpal unit both under the dentinal tubes sectioned by the preparation of some Class V cavities and on the opposite side of the pulp chamber, independent of tooth preparation.

The conclusion of the study was that the odontoblast layer at the base of the dentin did not change after the cavities were performed, being identical to the one below the normal dentin, without lesions.

Our study analyzed the changes that occurred in the structure of the dentinal tubules after the decay. The main changes we observed are their obliteration in the external third, which include the distal portion of the extension of the odontoblasts, thus determining their "shortening". Farges *et al.* [8] detailed the complex response of odontoblasts to pathogens and their ability to withstand caries attack through a cellular immune response. This response depends on Toll-like receptors (TLRs) found in odontoblasts. Those receptors could detect potential pathogens. Their study exemplifies the activity of cells from a biochemical point of view, compared to our study that addresses structural changes.

Szabó *et al.* demonstrated the presence of the extensions in all three areas of dentin, using the electron microscope [9]. The difference between our study and theirs lies in the analysis carried out by Szabó *et al.* on the ramifications of these extensions. By analyzing the healthy specimens, we demonstrated the presence of the extensions at the DEJ level and in the external third of the dentin. Sigal *et al.* also demonstrated the presence of the extensions at DEJ level, using scanning electron microscopy (SEM) to analyze the length and morphology of the odontoblastic extension on the dentinal surface of some demineralized and previously prepared teeth. Using immunofluorescence marking of tubulin, they highlighted the odontoblastic extensions from their cell bodies to DEJ, some of them also exhibiting terminal and lateral extensions. The presence of tubulin-containing structures extending up to DEJ supports the hypothesis that the structures observed with SEM are odontoblastic processes [10].

On the other hand, Goracci *et al.* wanted to demonstrate, with the help of confocal laser scanning microscopy (CLSM), the exact area to which these processes extend [11]. Field emission scanning electron microscopy (FE-SEM) provided additional evidence that the tubular structures are visible only in the inner third of the dentin, towards the pulp.

Samples affected by carious process in our study included sclerotic dentin. Stanley *et al.* observed the complex response of the dental pulp to external stimuli by correlating the defense capacity of the pulp with the patient's age/gender, the type and location of the surface of the dental lesions by sectioning the tissue, through micro-radiography and by descaling sections embedded in paraffin. The number of samples was higher compared to our study, including 270 teeth extracted. They noted [12] that this response of the pulp–dentin complex to stimuli of a carious or traumatic nature is manifested by depositing sclerotic dentin, repair dentin and then by creating "dead paths" (also observed in our study).

Bjørndal *et al.* study described cellular and micro-radiographic examination on thin non-demineralized enamel–dentin sections performed on 36 enamel lesions from freshly extracted third molars [13]. The activity of the lesions was determined by clinical examination and by the estimated age of the lesion at the time of extraction. Cellular reactions to lesions of the enamel–dentin complex were measured histomorphometrically following the subsequent conditions: (*i*) nucleus/cytoplasm ratio of the odontoblast; (*ii*) the odontoblast/dentin tubule ratio; (*iii*) the area of the adjacent predentin (μm^2). The difference between our study and that of Bjørndal *et al.* is represented by the analysis of the changes that occurred within the odontoblast throughout the active lesions. The length of the tubules may be compared with the length of odontoblast processes [14]. This might explain the difference we obtained between the healthy and altered dental tissues in respect to the odontoblastic processes reaching DEJ.

As a comparison, at the cemento–enamel junction, the dentin tubule density is relatively uniform for 1–2 mm, and increases from the outer surface inwards, according to Komabayashi *et al.* [15].

Another aspect worth mentioning is the demineralization consequence on dentin resistance. As pointed out by Georgescu *et al.*, a sclerotic dentin would present a significant higher resistance to acid etching using regular 37% *ortho*-phosphoric acid [16]. On the other hand, dental treatments would influence the dentin color by infusing the very dentinal tubules, especially in the cervical third of the crown [17]. Other materials also exhibit different adhesion affinities for normal and sclerotic dentin, resulting in a lower thickness of hybrid layer in an affected dentin [18], in accordance with the decrease in open tubules we also noted in the current study. We should consider the possible contribution to pressure modifications at the DEJ upon fluidic content of dentinal tubules of orthodontic forces on the brackets and transmitted to the enamel [19], as well as excess bleaching agents on enamel surface [20].

The density of dentinal tubules might be influenced by preexisting conditions, such as hyperbilirubinemia [21], by adhesion techniques used for composite materials [22]

or by using arginine-containing dentifrice that would obliterate them to help patients with dentin hypersensitivity [23, 24].

Since occlusal trauma leads to morphological changes of dental pulp, as pointed out by Cărămizaru *et al.* [25], it might also yield modification in dental tubules orientation and permeability, an aspect we have not assessed in this particular study.

⯐ Conclusions

In our study, we have observed the differences between the coronal healthy tissues and those altered by the carious process, and we have noted the presence of the odontoblast process in the inner dentin as well as near DEJ. With the help provided by the analysis software, we have objectivated the reduction of the number of the processes reaching DEJ in case of a carious lesions, and in some areas, their gradual decrease. The number of tubules containing odontoblastic processes that reach DEJ is decreased in teeth with caries. Obliteration of dentin tubules might be explained by intratubular deposition of tertiary dentin, leading to the reduced detectable number of odontoblastic processes in the analyzed samples. Our proposed method for assessing the number of odontoblast processes is an easy, accessible one, that might be used by several professionals in the field. This study is consistent with the data found in literature and addresses a different way of appreciating the changes that take place in dentin throughout the carious process. A possible follow-up could be represented by the analysis of different reaction of the odontoblast in response to the various stages of dental caries evolution – from the superficial enamel-only involvement to a complicated decay, with partial/total interest of the pulp chamber.

Conflict of interests

The authors declare that they have no conflict of interests.

Authors' contribution

All authors of this research paper have directly participated in the planning, execution, or analysis of this study, and also all authors of this paper have read and approved the final version submitted.

Acknowledgments

The authors would like to thank Eng. Radu Matei for his much appreciated help in this study.

References

[1] Featherstone JDB. Dental caries: a dynamic disease process. Aust Dent J, 2008, 53(3):286–291. https://doi.org/10.1111/j.1834-7819.2008.00064.x PMID: 18782377

[2] Iliescu A, Gafar M. Cariologie şi odontoterapie restauratoare. Medical Publishing House, Bucharest, 2001 [in Romanian]. https://www.ed-medicala.ro/135-cariologie-si-odontoterapie-restauratoare-andrei-iliescu-memet-gafar.html

[3] Fejerskov O, Kidd E (eds). Dental caries: the disease and its clinical management. 2nd edition, Wiley–Blackwell Publishing, Oxford, UK, 2008. https://www.wiley.com/en-au/Dental+Caries%3A+The+Disease+and+Its+Clinical+Management%2C+2nd+Edition-p-9781118068908

[4] Popa MB, Bodnar DC, Vârlan CM, Velcescu C, Suciu I. Manual de odontoterapie restauratoare. Carol Davila University Publishing House, Bucharest, 2007 [in Romanian]. https://

[5] www.worldcat.org/title/manual-de-odontoterapie-restauratoare/oclc/895192236

[5] Maniatopoulos C, Smith DC. A scanning electron microscopic study of the odontoblast process in human coronal dentine. Arch Oral Biol, 1983, 28(8):701–710. https://doi.org/10.1016/0003-9969(83)90104-8 PMID: 6579902

[6] Brännström M, Garberoglio R. The dentinal tubules and the odontoblast processes. A scanning electron microscopic study. Acta Odontol Scand, 1972, 30(3):291–311. https://doi.org/10.3109/00016357209004598 PMID: 4510760

[7] Murray PE, About I, Lumley PJ, Franquin JC, Remusat M, Smith AJ. Human odontoblast cell numbers after dental injury. J Dent, 2000, 28(4):277–285. https://doi.org/10.1016/s0300-5712(99)00078-0 PMID: 10722902

[8] Farges JC, Keller JF, Carrouel F, Durand SH, Romeas A, Bleicher F, Lebecque S, Staquet MJ. Odontoblasts in the dental pulp immune response. J Exp Zool B Mol Dev Evol, 2009, 312B(5):425–436. https://doi.org/10.1002/jez.b.21259 PMID: 19067439

[9] Szabó J, Trombitás K, Szabó I. The odontoblast process and its branches in human teeth observed by scanning electron microscopy. Arch Oral Biol, 1984, 29(4):331–333. https://doi.org/10.1016/0003-9969(84)90108-0 PMID: 6586129

[10] Sigal MJ, Pitaru S, Aubin JE, Ten Cate AR. A combined scanning electron microscopy and immunofluorescence study demonstrating that the odontoblast process extends to the dentinoenamel junction in human teeth. Anat Rec, 1984, 210(3):453–462. https://doi.org/10.1002/ar.1092100306 PMID: 6395720

[11] Goracci G, Mori G, Baldi M. Terminal end of the human odontoblast process: a study using SEM and confocal microscopy. Clin Oral Investig, 1999, 3(3):126–132. https://doi.org/10.1007/s007840050090 PMID: 10803123

[12] Stanley HR, Pereira JC, Spiegel E, Broom C, Schultz M. The detection and prevalence of reactive and physiologic sclerotic dentin, reparative dentin and dead tracts beneath various types of dental lesions according to tooth surface and age. J Oral Pathol, 1983, 12(4):257–289. https://doi.org/10.1111/j.1600-0714.1983.tb00338.x PMID: 6193259

[13] Bjørndal L, Darvann T, Thylstrup A. A quantitative light microscopic study of the odontoblast and subodontoblastic reactions to active and arrested enamel caries without cavitation. Caries Res, 1998, 32(1):59–69. https://doi.org/10.1159/000016431 PMID: 9438573

[14] Charadram N, Austin C, Trimby P, Simonian M, Swain MV, Hunter N. Structural analysis of reactionary dentin formed in response to polymicrobial invasion. J Struct Biol, 2013, 181(3):207–222. https://doi.org/10.1016/j.jsb.2012.12.005 PMID: 23261402 PMCID: PMC3578079

[15] Komabayashi T, Nonomura G, Watanabe LG, Marshall GW Jr, Marshall SJ. Dentin tubule numerical density variations below the CEJ. J Dent, 2008, 36(11):953–958. https://doi.org/10.1016/j.jdent.2008.08.002 PMID: 18786756 PMCID: PMC2597416

[16] Georgescu A, Iovan G, Stoleriu S, Topoliceanu CI, Andrian S. Atomic force microscopy study regarding the influence of etching on affected and sclerotic dentine. Rom J Morphol Embryol, 2010, 51(2):299–302. PMID: 20495747

[17] Suciu I, Ionescu E, Dimitriu BA, Bartok RI, Moldoveanu GF, Gheorghiu IM, Suciu I, Ciocîrdel M. An optical investigation of dentinal discoloration due to commonly endodontic sealers, using the transmitted light polarizing microscopy and spectro-photometry. Rom J Morphol Embryol, 2016, 57(1):153–159. PMID: 27151701

[18] Florescu A, Efrem IC, Haidoiu C, Hertzog R, Bîcleşanu FC. Microscopy comparative evaluation of the SE systems adhesion to normal and sclerotic dentin. Rom J Morphol Embryol, 2015, 56(3):1051–1056. PMID: 26662138

[19] Ciocan DI, Stanciu D, Popescu MA, Miculescu F, Plotog I, Vărzaru G, Ciocan LT. Electron microscopy analysis of different orthodontic brackets and their adhesion to the tooth enamel. Rom J Morphol Embryol, 2014, 55(2 Suppl):591–596. PMID: 25178330

[20] Dudea D, Florea A, Mihu C, Câmpeanu R, Nicola C, Benga Gh. The use of scanning electron microscopy in evaluating the effect of a bleaching agent on the enamel surface. Rom J Morphol Embryol, 2009, 50(3):435–440. PMID: 19690771

[21] Neves-Silva R, Alves FA, Antunes A, Goes MF, Giannini M, Tenório MD, Machado JL, Paes-Leme AF, Lopes MA, Santos-Silva AR. Decreased dentin tubules density and reduced thickness of peritubular dentin in hyperbilirubinemia-related green teeth. J Clin Exp Dent, 2017, 9(5):e622–e628. https://doi.org/10.4317/jced.53490 PMID: 28512537 PMCID: PMC 5429472

[22] Matei RI, Todor L, Cuc EA, Popescu MR, Dragomir LP, Rauten AM, Porumb A. Microscopic aspects of junction between dental hard tissues and composite material depending on composite insertion: layering *versus* bulk-fill. Rom J Morphol Embryol, 2019, 60(1):133–138. PMID: 31263837

[23] Lopes RM, Scaramucci T, Aranha ACC. Effect of desensitizing toothpastes on dentin erosive wear and tubule occlusion. An *in situ* study. Am J Dent, 2018, 31(4):177–183. PMID: 30106532

[24] Yuan P, Lu W, Xu H, Yang J, Liu C, Xu P. *In vitro* dentin tubule occlusion by an arginine-containing dentifrice. Am J Dent, 2019, 32(3):133–137. PMID: 31295394

[25] Cărămizaru M, Pleşea IE, Dragomir LP, Popescu MR, Uscatu CD, Şerbănescu MS, Alexandru DO, Comănescu TM. Quantitative assessment of morphological changes of dental pulp components of teeth affected by occlusal trauma. Rom J Morphol Embryol, 2018, 59(3):729–740. PMID: 30534811

Corresponding author
Horia Octavian Manolea, Professor, DMD, PhD, Department of Dental Materials, Faculty of Dentistry, University of Medicine and Pharmacy of Craiova, 2 Petru Rareş Street, 200349 Craiova, Dolj County, Romania; Phone +40766–335 216, e-mail: horia.manolea@umfcv.ro